

# Transient Stability of Synchronous Generator Connected to Micro Combined Heat and Power

Adel Hamad Rafa  
Tobruk University, Libya

**Abstract**— Micro Combined Heat and Power (Micro CHP) refers to small-scale installations that generate heat, electricity or both connected to the low voltage distribution network at the customer side. Although the connection of the Micro CHP to the low-voltage distribution networks improves security of supply, there are many operational challenges such as stability and control. This paper study the stability of synchronous generator connected to reciprocating engine as one type of Micro CHP. Also, a several studies have been done to investigate the response of Small scale embedded generation (SSEG) to a range of network faults and thereby ascertain the range of conditions under which SSEG might be expected to trip. Many of these may be regarded as nuisance trips when the action of network protection does not isolate the SSEG from a mains supply. Any protection associated with the SSEG has not been included in order to demonstrate inherent capability and response. The critical clearing time (CCT) is used to indicate the stability of the SSEG. In this investigation the CCT of the SSEG is calculated and simulated using Power Systems Computer Aided Design PSCAD/EMTDC as well as from the mathematical calculations.

**Index Terms:** Small scale embedded generation, Micro CHP, stability, synchronous generator.

## I. INTRODUCTION

Rising public awareness for environmental protection and continuously increasing energy consumption have created increased interest in distributed generation (DG) systems connected to the distribution network rather than the high voltage transmission network. Micro Combined Heat and Power (Micro CHP) takes the concept of distributed generation (DG), it is typically smaller generation at the point of use, and effectively eliminates the need to transport electricity from supplier to customer. Micro CHP systems are currently based on several different technologies: Reciprocating engines, Stirling engines, Micro gas turbines, and steam engines (Organic Rankin Cycle – ORC). While reciprocating engines are already commercially available, Stirling engines, ORC and micro-gas turbines are close to it with a substantial number of pilot and demonstration plants being in operation [1] [2].

Although there are many benefits in employing Micro CHP there are also many challenges with regards to stability, control and protection, to mention a few [3].

Traditional distribution network design did not need to consider issues of stability as the network was passive and remained stable under most circumstances. As the number of distributed generators connected to the main grid is rapidly increasing, the simultaneous disconnection of these distributed generators under fault conditions leads to local loads not being supplied by the distributed generation. This results in a decrease in system stability (i.e. angle and voltage stability) as hidden loads previously supplied by DGs, appears on the network.

Usually converting the mechanical power produced from Micro CHP systems (reciprocating engine, micro turbines...etc.) to electrical power by synchronous generators [4]. As the stability of the synchronous generator is defined as synchronous generator enables to remain in a state of operating equilibrium under normal operating conditions, and to regain an acceptable state of equilibrium after being subjected to a disturbance [5] [6]. Thus loss of stability leads to prevent the Micro CHP to provide reliable electricity and heat to the customers. Therefore this paper focuses on assessing the transient stability of a distribution network with synchronous generator connected to reciprocating engine in the event of faults at various locations in the network. The critical clearing time (CCT) is used to indicate the stability of the SSEG [7].

## II. RECIPROCATING ENGINES

Reciprocating engines are conventional internal combustion engines coupled with a generator and heat exchangers to recover the heat from the exhaust gas and the cooling cycle. Fig.1 shows the operation process of reciprocating engines that begins with fuel/air mixture is introduced into the combustion cylinder, and then compressed while the piston moves toward the top of the cylinder [4]. The heat from the engine exhaust, cooling water and oil jackets is used for respective heat demand. For micro combined heat and power (Micro CHP) applications, reciprocating engines offer low costs and good efficiency. However maintenance requirements are high and diesel-fuelled units have high emissions. Micro CHP products based on reciprocating engines are commercially available and are produced in large numbers by a variety of companies worldwide. The

Received 22 November 2017; revised 5 December 2017; accepted 6 December 2017.

Available online 1 January 2018.

market leader is the Germany based company Senertec (The Senertec model – called Dachs – generates around 5.5 kW and a thermal power of 14 kW). Other companies offering micro CHP products based on reciprocating engines include Power Plus, Spilling Energy System, Buderus, Oberdorfer and GE Jenbacher. Other companies from the Asian region offering micro CHP products are Honda (1 kW system – named Ecowill), Yanmar, Aisin and Sanyo. From the United States Victor Cogen is also developing a micro CHP system [8].

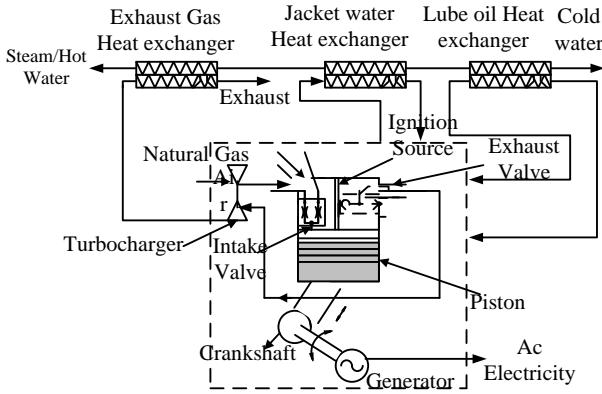


Figure 1. Process of Reciprocating Engines [4].

### III. TRANSIENT STABILITY STUDIES

The following studies present the investigation of the transient stability of a small diesel powered 11kVA three-phase synchronous generator connected to the LV cable network shown in Figure.2 A number of electrically local and remote three-phase faults have been applied and the critical clearance time (CCT) calculated. The studies are performed for two values of inertia constant ( $H = 1\text{ s}$  and  $1.7\text{ s}$ ) and simulation results are shown for fault clearance times in excess of the CCT to illustrate the impact of generator pole slipping. The figures in these studies illustrate the responses of the speed, load angle, and active and reactive powers of the machine, and also the voltage profile at the generator terminal and at the 0.433 kV and 11 kV bus bars. The impedance and time constants for the synchronous generators used in this work are obtained from Newage Stamford industrial generators data sheets [9].

#### A. LV Network Model for Fault studies

The network model used for the transient studies is shown as a single line diagram in Figure.2 and is based on an assumption of customers representing a suburban mix of residential dwellings and small commercial premises [10]. The high voltage (HV) 11kV network has been characterised using an ideal voltage source and impedance scaled to provide a fault level of 150MVA at the ring main unit (RMU) supplying the secondary substation. An impedance of 4.5% and rating of 0.5MVA have been taken for the secondary substation transformer. The demand on the secondary substation has been modelled as one detailed circuit and two equivalent

unbalanced loads with the values as shown (a uniform power factor of 0.95 lagging has been assumed) and short lengths of connecting cable.

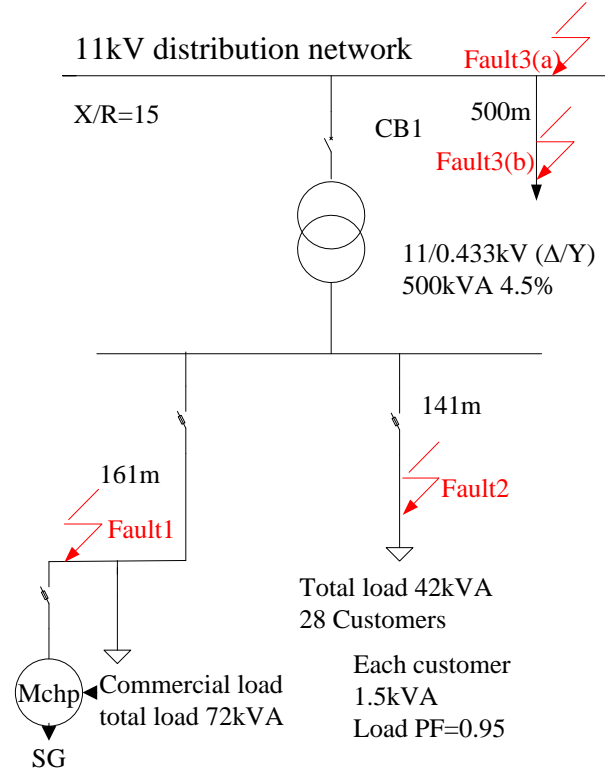


Figure 2. LV Network Model [10].

#### B. Fault 1: Within LV Commercial Premises

The CCT for a three-phase fault applied within the same commercial premises as the generator (Fault 1 in Figure.2) was found to be 90ms and 115ms for the inertia constant values of 1s and 1.7s respectively. As shown in Figure.3, (b) to (c), the duration of the fault is 110 ms applied at 3s (the complete collapse of voltage can be observed), in this case the generator ( $H=1.7\text{ s}$ ) recovers stability once the fault is cleared and returns to the pre-fault operating condition. If the duration of the fault is larger than the  $CCT=110\text{ ms}$  the generator will not recover stability after fault clearance.

Figure.4 illustrates the instability of the generator ( $H=1.7\text{ s}$ ) by showing the machine internal angle, load angle and shaft speed responses for a fault duration of 116 ms applied at 3s. During the fault the speed increases to high speed and, depending on the mechanical design, could cause damage if the generator is not quickly tripped. The onset of instability can be observed after the continual increase in machine angle after the fault clearance the generator pole-slips. However, as faults within the commercial premises will be quickly cleared by the substantial fault current contribution from the mains supply, instability arising from these events is not deemed to be of concern.

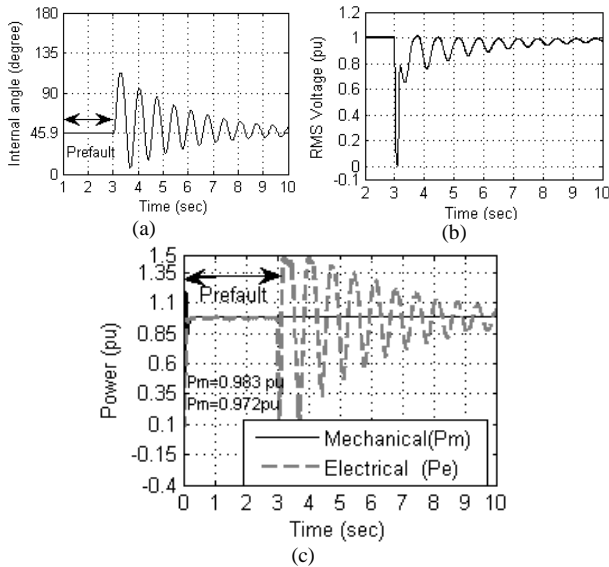


Figure 3. Performance of (SG) During LV Local Three-Phase Fault ( $t_c = 110$  ms): (a) Machine Internal Angle, (b) Terminal Voltage & (c) Mechanical and Electrical Power.

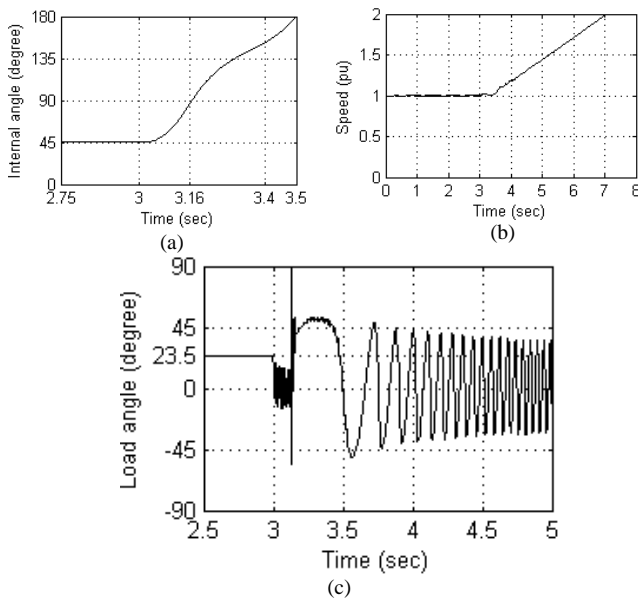


Figure 4. Performance of (SG) During LV Local Three-Phase Fault ( $t_c = 116$  ms): (a) Machine Angle, (b) Shaft Speed & (c) Load Angle.

C. Fault 2: Adjacent LV Circuit

The fault was applied on an adjacent LV circuit (Fault 2 in Figure.2) and it was observed that instability did not occur due to the relatively high retained voltage at the generator terminals. As an example, Figure.5 shows the machine angle, shaft speed, terminal voltage responses and active and reactive powers of the machine for a fault duration of 500ms applied at 3s ( $H = 1.7s$ ). The power angle returned to the pre-fault value and the speed increased to 1.009 pu, but the voltages at the generator terminals and the load terminals decreased to 0.85 pu and 0.77 pu respectively (voltage sag). As shown in the results this voltage sag has an effect on the active and reactive power of the generator. The purpose of applying

such a long-duration fault was to explore the performance of the generator during a permanent fault (assuming protection system failure). It also can be observed that when the fault is located further away from the generator it will evidently have the capability of withstanding faults of larger duration.

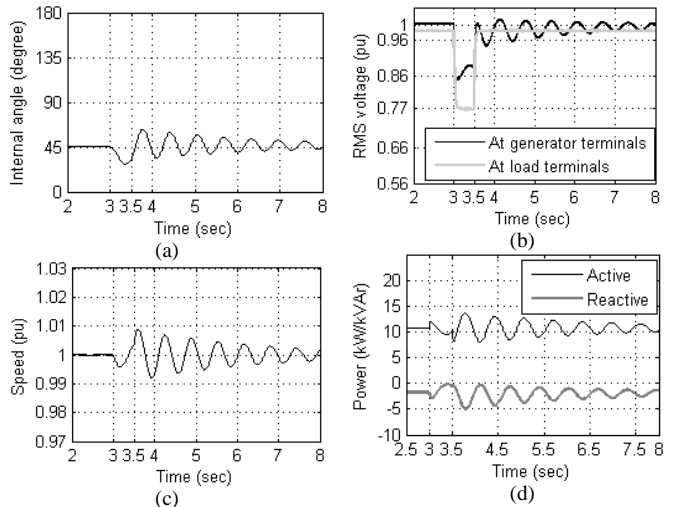


Figure 5. Performance of (SG) During Adjacent LV Circuit Fault: (a) Machine Angle, (b) Generator and Load Terminal Voltages (c) Shaft Speed & (d) Active and Reactive Power.

D. Fault 3: Electrically Remote on HV Distribution Network

Two specific fault conditions were applied on the HV side of the secondary substation and the CCT of the machine was found for both cases with different inertia constants. The first fault condition was when a three-phase fault occurred adjacent to the HV terminals of the secondary substation transformer and the second when the same fault occurred at a remote location on the HV cable circuit.

For the first condition the CCTs were calculated as being 82ms and 110ms for the inertia constant values of 1s and 1.7s respectively. For the second condition the fault was placed 500m along a length of cable and the CCTs were found to be equal to 91ms and 121ms. Fig.6 (a) and (b) illustrate the instability of the machine for a fault adjacent to the HV terminals with the drop in terminal voltage again evident. Figure.6 (a) shows the internal machine angle as function of time, for the three values of fault clearing time ( $t_c$ ): 100ms, 110 ms (critical clearing time) and 112 ms. The critical clearing angle ( $\delta_{cr}$ ) is about  $70^\circ$ . The results show that, when the fault duration is larger than the CCT the generator loses stability.

E. The Relationship between the Inertia, Fault Location and CCT

This study aims to show the relationship between the generator inertia, fault location and CCT. A number of electrically local and remote three-phase faults have been applied, and the critical clearance time (CCT) calculated.

The studies are performed for different values of combined inertia constant (H) of the generator and prime mover (H = 1s, 1.35s and 1.7s). Figure.7 shows the relationship between the CCT, inertia constant of the machine and fault location. The results show that, the CCT increases as the inertia of the machine becomes larger showing a practically linear relationship. Also it was observed that the location of the fault (in the case of HV fault) significantly affected the CCT. The generator in case of the HV Distribution Network (500m) has longer CCT than in case of the HV transformer terminal fault.

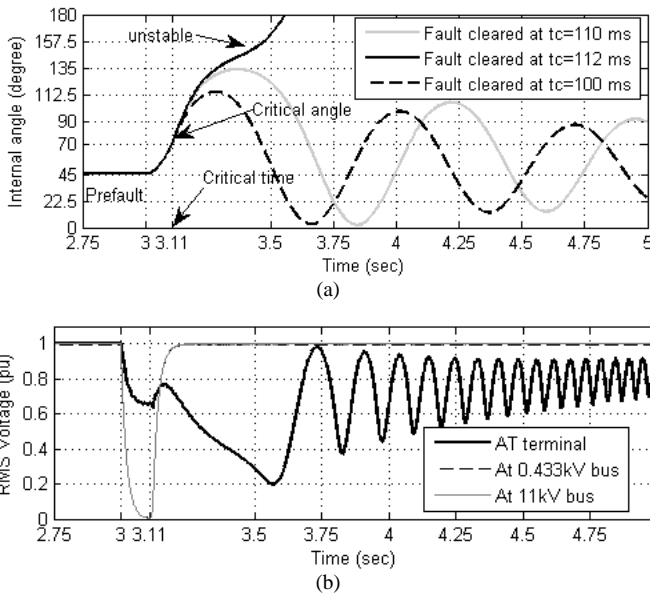


Figure 6. Performance of (SG) During Remote HV Fault: (a) Machine Internal Angle Response for Different Values of Fault Clearing Time & (b) Terminal, 11kVbus and 0.433 kV Bus Voltages.

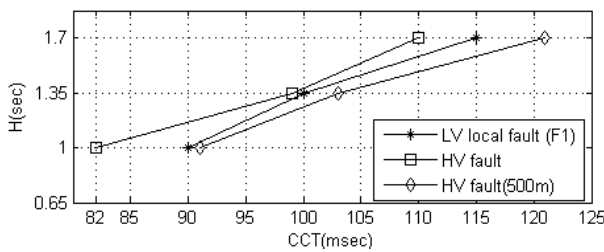


Figure 7. Relationship between Inertia Constant, Fault Location and CCT.

#### IV. THEORETICAL RESULT

The function of this calculation is to compare the simulation results with the calculation results to examine the models that implemented in the software and provide an evidence to the readers to be convince to the software result. The critical angle and critical time for the synchronous generator have been calculated by using circuit analysis and machine theory.

#### A. The Equivalent Circuit of the Distribution Network

Calculating the critical angle and critical speed requires calculating the circuit impedance between the generator and the infinite bus, the voltage at the bus where the generator is connected to. Fig.8 shows the equivalent circuit of the low voltage network used in this study (Fig.2).

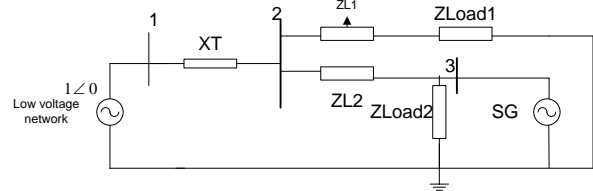


Figure 8, Network Impedances Diagram

Where  $Z_{L1}$ ,  $Z_{Load1}$ ,  $Z_{L2}$  and  $Z_{Load2}$  are the impedance of lines 1 and 2 as well as load1 and 2 respectively. XT is transformer reactance.

The impedances values will be converted to per unit values on the system base. In general, the per unit value is the ratio of the actual value and the base value of the same quantity[11].

$$\text{per unit value} = \frac{\text{actual value}}{\text{base value}} \quad (1)$$

For the system the generator voltage and power have been taken as the system base (11kVA, 0.433kVA). The base impedance  $Z_{base}$  is given by:

$$Z_{base} = \frac{V_{base}^2}{S_{base}} \quad [11] \quad (2)$$

$$S_{base} = 11 \text{ kVA}$$

$$V_{base} = 433 \text{ V}$$

$$Z_{base} = \frac{V_{base}^2}{S_{base}} = \frac{433^2}{11000} = 17.044 \Omega$$

The impedance of line 1 ( $Z_{L1}$ ) and load1 ( $Z_{Load1}$ ) in per unit are:

$$Z_{L1 p.u.} = \frac{Z_{L1}}{Z_{base}} = \frac{0.0323 + j0.0110929}{17.044} = 0.00194 + j0.00057 \text{ p.u.}$$

$$Z_{Load1 p.u.} = \frac{Z_{Load1}}{Z_{base}} = \frac{4.067 + j1.268}{17.044} = 0.2387 + j0.0744 \text{ p.u.}$$

The impedance of line 2 ( $Z_{L2}$ ) and load2 ( $Z_{Load2}$ ) in per unit are:

$$Z_{L2 p.u.} = \frac{Z_{L2}}{Z_{base}} = \frac{0.0376 + j0.0097}{17.044} = 0.0022 + j0.00065 \text{ p.u.}$$

$$Z_{Load2 p.u.} = \frac{Z_{Load2}}{Z_{base}} = \frac{2.474 + j0.813}{17.044} = 0.1451 + j0.0477 \text{ p.u.}$$

Converting the transformer reactance from the transformer per unit to the system per unit is given by:

$$Z_{N \text{ p.u.}} = Z_{M \text{ p.u.}} \frac{MVA_{N \text{ base}} \cdot (kV_{M \text{ base}})^2}{MVA_{M \text{ base}} \cdot (kV_{N \text{ base}})^2} \quad [11] \quad (3)$$

Where the old base and per unit values of the transformer are denoted by subscript M, the base values of the system are denoted by subscript N. Thus the new per unit value is:

$$Z_{N \text{ p.u.}} = 0.045 \times \frac{0.011 \cdot (0.433)^2}{0.5 \cdot (0.433)^2} = 9.9 \times 10^{-4} \text{ pu}$$

The Thevenin equivalent of the network, as viewed from the generator terminals, is shown in Fig.9.

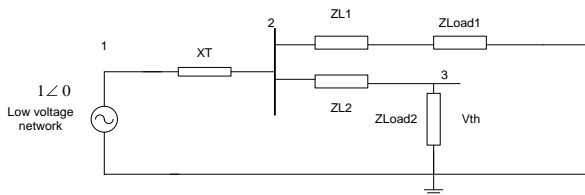


Figure 9. The Network Equivalent Circuit after Disconnecting the Generator

The Thevenin voltage is the voltage on bus 3 ( $V_{th} = V_3$ ). The voltage at bus 3 can be calculated by using Kirchhoff current law as follow:

$$\begin{bmatrix} -j1010 & j1010 & 0 \\ j1010 & -421.8 + j1134.8 & 418 - j123.5 \\ 0 & 418 - j123.51 & -424.2 + j125.59 \end{bmatrix} \begin{bmatrix} V1 \\ V2 \\ V3 \end{bmatrix} = \begin{bmatrix} 0 \\ -j1010.1 \\ 0 \end{bmatrix}$$

The voltage at bus 1 is known then the first row and the first column are eliminated from the matrix.

$$\begin{bmatrix} -421.8 + j1134.8 & 418 - j123.5 \\ 418 - j123.5 & -424.2 + j125.59 \end{bmatrix} \begin{bmatrix} V2 \\ V3 \end{bmatrix} = \begin{bmatrix} -j1010.10 \\ 0 \end{bmatrix}$$

$$V3 = \frac{\begin{bmatrix} -421.8 + j1134.8 & -j1010.10 \\ 418 - j123.5 & 0 \end{bmatrix}}{\begin{bmatrix} -421.8 + j1134.8 & 418 - j123.5 \\ 418 - j123.51 & -424.2 + j125.59 \end{bmatrix}} = \frac{1.2475e + 005 + 4.2222e + j005}{-1.2306e + 005 - 4.3111e + j005}$$

$$V3 = 0.9814 \angle -0.53^\circ \text{ pu}$$

Thevenin impedance is:

$$Z_{33} = [X_T // (Z_{L1} + Z_{Load1}) + Z_{L2}] // Z_{Load2} \quad (4)$$

Or it can be found from the Z bus ( $Z_{33}$ ) of the network after the generator is disconnected from the circuit. The  $Z_{33}$  is the impedance of bus 3 where the generator is connected to the network which can be calculated by

finding the Y bus first then the inverse of the Y bus is the Z bus.

The Y bus matrix of the system is:

$$Y = \begin{bmatrix} -421.8 + j1134.8 & 418 - j123.5 \\ 418 - j123.5 & -424.2 + j125.59 \end{bmatrix}$$

By taking the inverse of the Y bus the Z bus is:

$$Z = \begin{bmatrix} 0.0000 + j0.0010 & 0.0000 + j0.0010 \\ 0.0000 + j0.0010 & 0.0022 + j0.0016 \end{bmatrix}$$

From the Z matrix ( $Z_{33}$ ) as well as from the parallel and series calculations the value of the Thevenin impedance of the network is:

$$Z_n = Z_{33} = R_{33} + jX_{33} = 0.0022 + j0.0016 \text{ pu}$$

Fig.10 shows the Thevenin equivalent of the distribution network.

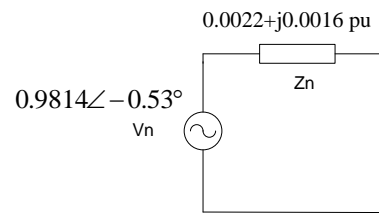


Figure 10. The thevenin equivalent of the network.

### B. Calculation of Critical Clearing Angle/time

In order to compare the simulation results with the mathematical result for finding the critical angle ( $\delta_{cr}$ ) and critical clearing time (CCT) for the synchronous generator considered in this study the equal-area criterion method has been used. Calculating the critical angle requires calculating the reactance between the generator internal voltage and the network, mechanical power ( $P_m$ ) and electrical power ( $P_e$ ). Figure.11 shows the generator equivalent circuit connected to the network.

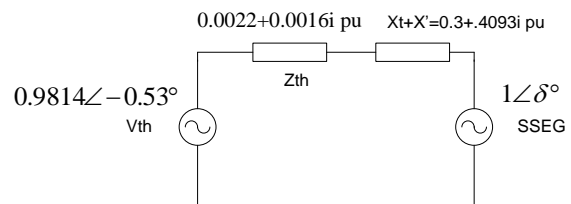


Figure 11. The Equivalent Circuit of the Synchronous Generator and the Network

Where

$X'$  is the transient reactance of the generator which is equal to 0.3 pu.

$X_t$  is reactance between the network and the generator  $6.97\Omega$  (22.2 mH). It is used for transmitting 11kW at corresponding phase angle difference equal to 23.3 deg. (0.406 rad) as clearly satisfied from the simulation results

as shown in Figure.4 this is entered as the initial machine angle for initialization. The per-unit reactance  $X_t$  is calculated by:

$$X_{p.u.} = \frac{X_t}{Z_{base}} = \frac{6.97}{17.044} = 0.4093 \text{ p.u.} \quad (5)$$

Figure. 12 shows the  $p-\delta$  plot. At steady state, the value of the electrical power of the generator is ( $P_e$ ) 0.972 pu and the mechanical input torque of the generator ( $P_m$ ) is 0.983 pu.

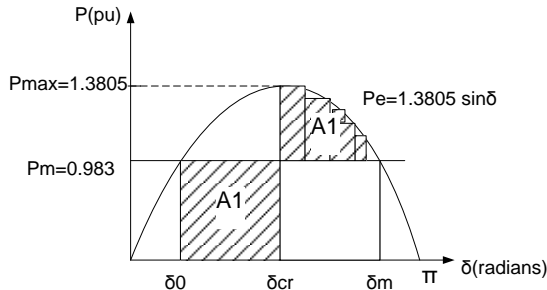


Figure 12.  $p-\delta$  Plot for Case Study [3].

The value of  $R_{33}$  and the Thevenin voltage angle are ignored to make this calculation easier. The power supplied by the generator is:

$$P_e = \frac{V_g V_{SE}}{X' + X_t + X_{33}} \sin \delta_0 \quad [5] \quad (6)$$

$$P_e = \frac{0.9814 \times 1}{0.3 + .4093 + .0016} \sin \delta_0$$

$$P_e = 1.3805 \sin \delta_0$$

The value of  $P_e=0.972$  pu thus the steady state the internal phase angle  $\delta_0$  is  $44.76^\circ = 0.7813$  radians.

In this study the disturbance is a temporary three-phase fault on the grid side of the low voltage network. The power angle then increases to a maximum value  $\delta_m = 180 - \delta_0 = 135.24^\circ = 2.3603$  radians, which gives the maximum decelerating area. Equating the accelerating and decelerating areas in the  $p-\delta$  plot:

$$A1=A2$$

$$A1 = \int_{\delta_0}^{\delta_{cr}} p_m d\delta = A2 = \int_{\delta_{cr}}^{\delta_m} (P_{max} \sin \delta - p_m) d\delta \quad [5] \quad (7)$$

$$\int_{0.7813}^{\delta_{cr}} 0.983 d\delta = \int_{\delta_{cr}}^{2.3603} (1.3805 \sin \delta - 0.983) d\delta$$

Solving for  $\delta_{cr}$

$$0.983 \times (\delta_{cr} - 0.7813) = 1.3805[\cos \delta_{cr} - \cos(2.3603)] - 0.983 \times (2.3603 - \delta_{cr})$$

$$1.3805 \cos \delta_{cr} = 0.572$$

$$\delta_{cr} = 1.1435 \text{ radians} = 65.52^\circ$$

To calculate the critical clearing time (CCT) the swing equation is integrated twice with initial condition

$$\delta_{cr}(0) = \delta_0 \text{ and } \frac{d\delta(0)}{dt} = 0,$$

$$\frac{2H}{\omega_{syn}} \frac{d\delta(0)}{dt} = pm \text{ pu} \quad [12] \quad (8)$$

$$\frac{d\delta(t)}{dt} = \frac{(\omega_{syn})(pm, pu)}{2H} t + 0 \quad (9)$$

$$\delta(t) = \frac{(\omega_{syn})(pm, pu)}{4H} t^2 + \delta_0 \quad (10)$$

Solving

$$t = \sqrt{\frac{4H}{\omega_{syn} P_{mpu}} (\delta(t) - \delta_0)} \quad [12] \quad (11)$$

Then the critical clearing time for inertia constant ( $H=1s$  and  $H=1.7s$ ) is:

$$t = \sqrt{\frac{4(H)}{100\pi \times (.983)} (1.1435 - 0.7813)}$$

Table 1 shows the simulation and calculation results for different CCT for various inertial constants.

Table 1.. Different CCT for various inertial constants

Method	Steady state angle ( $\delta_0$ ) (degree)	Critical angle ( $\delta_{cr}$ ) (degree)	CCT (ms)	
			H (s)=1	H (s)=1.7
Simulation Results	45.9°	70°	82	110
Calculation Results	44.76°	65.52°	69	90

## V. CONCLUSIONS

This paper presents the results of studies concerning the transient behavior of small synchronous generator connected to Micro CHP in response to network transients. The results of case studies developed to examine the impact of fault locations, typical clearance times and type of fault (symmetrical or asymmetrical) on the critical clearance times of synchronous generator are presented. The results show that the stability of the synchronous generator during a disturbance depended on the rotor angle stability which is concerned with the ability of the synchronous generator to remain in synchronism with the network. Concerning the type of fault, it was observed that the three-phase fault is more less severe on the generator than a single-phase to ground fault. Moreover the grid fault contribution at LV ensures fast fault clearance by operating the various fuses located on the network and consequently the tripping of synchronous generator due to instability will not occur except in the cases where the fault is either at the terminals or in the service connection (sufficient terminal voltage remains for the electrically remote LV faults). Furthermore the studies are complemented by finding the

relationship between the inertia of the synchronous generator, fault location and CCT. Also the theoretical results are close to simulation results, which give evidence of the software validation

Finally from this investigation it has been found that the stability of the network may be endangered due to the small inertia of the synchronous generator. More care is required to ensure that the generator does not trip for remote network faults; otherwise, the heat energy and the electrical energy from micro CHP in the building may be lost.

## REFERENCES

- [1] National Energy Regulator of South Africa, "Small-Scale Embedded Generation: Regulatory Rules Consultation Paper", 25 February 2015.
- [2] Saeed Jahdi, Loi Lei Lai, Daneil Nankoo, Renewable Hybrids Grid-Connection Using Converter Interferences, International Journal of Sustainable Energy Development (IJSED), Volume 2, Issue 1, June 2013
- [3] TamilSelvi B, Maharaja K, Shankar C.K and Leo Sekar G, "Optimal Allocation of Distributed Energy Source for inter connected Operation of Microgrid," 4th National Conf. on Frontiers in Applied Sciences and Computer Technology (FACT'16), March 18& 19, 2016 Vol.04 PP: 24-27, 2016.
- [4] G. R. Simader, R. Krawinkler and G. Trnka, "Micro CHP systems state-of-the-art," Final Report, Vienna, March 2006.
- [5] P. Kundur, "Power System Stability and Control (book)", McGraw-Hill Inc., 1994.
- [6] N. Hatziaargyriou, M. Donnelly, S. Papathanassiou, J.A. Pecas Lopes, M. Takasaki, H. Chao, J. Usaola, R. Lasseter, A. Efthymiadis, K. Karoui, S. Arabi, "Modeling New Forms of Generation and Storage," CIGRE TF38.01.10, November 2000.
- [7] X. Wu, Y. Zhang, A. Arulampalam, N. Jenkins, "Stability of Large Scale Integration of Micro Generation into Low Voltage Grids," International Journal of Distributed Energy Resources, Vol. 1, December 2005, pp 1614-7138.
- [8] US Department of Energy Office of Energy Efficiency and Renewable Energy, "Advanced Micro turbine systems Program Plan for Fiscal Years 2000 Through 2006", Tech .Rep, 2006.
- [9] Available at: [www.newage-avkse.com](http://www.newage-avkse.com)
- [10] S. Ingram, S. Probert, K. Jackson, "The Impact of Small Scale Embedded Generation on the Operating Parameters of Distribution Networks", Contractor PB Power, DTI Renewable.
- [11] Mohamed E. El-Hawary, Electrical Energy Systems(book), Dalhousie University, CRC Press LCC, Boca Raton London ,New York and Washington, D.C.,2000.
- [12] J. Thomas Overbye, Duncan Glover, Mulukutla S. Sarma, Power Systems Analysis and Design (book), 4th ed ,CL-Engineering,2007

## BIOGRAPHIES



**Dr. Adel Hamad Rafa** (Assistant Professor ) received the B. Eng. from Garuonise University, Libya, and M.Sc. degrees from University Putra Malaysia, , and the Ph.D. degree from University of Strathclyde, Glasgow, UK in 19991 ,2003 and 2010, respectively. He worked in Tobruk Power Station, 1992-1995; (2012-2017) He was dean of the Faculty of Engineering Tobruk University, Libya. His research interests include protection, electric machines and renewable energy technologies.